Received 22.04.2025 Revised 30.07.2025 Accepted 23.09.2025

Vol. 21, No. 5
2025

Scientific Reports of the National University of Life and Environmental Sciences of Ukraine

Journal homepage: https://scireports.com.ua/en

UDC 514.18

Doi: 10.31548/dopovidi/5.2025.114

Calculation of a gravitational screw chute with an axial cross-section curve defined by an explicit equation

Serhii Pylypaka
Doctor of Technical Sciences, Professor
National University of Life and Environmental Sciences of Ukraine
03041, 15 Heroiv Oborony Str., Kyiv, Ukraine
https://orcid.org/0000-0002-1496-4615

Tetiana Volina*
Doctor of Technical Sciences, Associate Professor
National University of Life and Environmental Sciences of Ukraine
03041, 15 Heroiv Oborony Str., Kyiv, Ukraine
https://orcid.org/0000-0001-8610-2208

Victor Nesvidomin
Doctor of Technical Sciences, Professor
National University of Life and Environmental Sciences of Ukraine
03041, 15 Heroiv Oborony Str., Kyiv, Ukraine
https://orcid.org/0000-0002-1495-1718

Vitaliy Babka
PhD in Technical Sciences, Associate Professor
National University of Life and Environmental Sciences of Ukraine
03041, 15 Heroiv Oborony Str., Kyiv, Ukraine
https://orcid.org/0000-0003-4971-4285

Taras Pylypaka
PhD in Technical Sciences, Associate Professor
National University of Water and Environmental Engineering
33028, 11 Soborna Str., Rivne, Ukraine
https://orcid.org/0009-0000-5582-1859

Abstract. Screw gravity chutes are used for energy-free transportation of cargo and gravitational separation of ores, which necessitates an optimal combination of design parameters of the working surface, speed of movement, and compactness of the trajectory. The aim of the work was to analytically describe the movement of a cargo along a screw surface, given by the curve of its axial

Suggested Citation:
Pylypaka, S., Volina, T., Nesvidomin, V., Babka, V., & Pylypaka, T. (2025). Calculation of a gravitational screw chute with an axial cross-section curve defined by an explicit equation. *Scientific Reports of the National University of Life and Environmental Sciences of Ukraine*, 21(5), 114-128. doi: 10.31548/dopovidi/5.2025.114.

*Corresponding author

cross-section, under the action of its own weight, using the example of a material particle. Methods of classical mechanics, differential surface theory and numerical methods were used to solve the problem. The main results of the study were based on the fact that after stabilising its motion, the material particle begins to slide along the surface at a constant speed and a constant distance from the axis of the helical surface, taking into account the shape of the curve of its axial cross-section. It was established that the equation of this curve may include constant values that affect its shape, i.e., the kinematic parameters of the particle. This made it possible to find the required values of the constants to ensure the specified parameters of particle sliding. The differential equations of motion of a particle sliding along a helical surface were compiled in projections on the axes of a stationary coordinate system. A parabola was considered as the curve of the axial cross-section of the surface, the equation of which includes a constant value. The obtained analytical dependencies made it possible to determine the optimal values of the constants in the equation of the axial cross-section curve, which ensured the required sliding speed of the particle and the distance from the axis of the helical surface. This opened up opportunities for designing screw chutes taking into account specific technological requirements, in particular for gravitational separation or energy-free transportation of bulk materials. The practical application of the proposed calculations is demonstrated by the example of a parabolic cross-section, which confirms the effectiveness of the method for optimising the kinematic parameters of motion. As a result of the study, expressions for the design of screw gravity chutes were obtained and the influence of the introduced constant on the kinematic parameters of particle sliding was determined

Keywords: sliding velocity; gravitational forces; reactions; friction; gravitational transportation

Introduction

Screw gravity chutes are widely used for energy-free transportation of bulk and piece goods, as well as in the mining industry for mineral enrichment by gravity separation. Their use reduces energy consumption and increases the reliability of transport systems, but the efficiency of such chutes depends largely on the design parameters of the working surface, the speed of the material and its sliding trajectory. Incorrectly selected geometric characteristics can lead to damage to the cargo or loss of separation efficiency. The shape of the axial cross-section of the screw surface plays a special role, as it determines the kinematic parameters of particle movement, its speed and distance from the axis. The selection and analytical justification of these parameters is a pressing issue, as it ensures the reliability of transportation and the stability of technological processes without additional energy costs.

Screw surfaces are the subject of research by scientists in many fields. V. Bulgakov *et al.* (2023) investigated the power and load parameters of flexible screw conveyors, in particular for the transportation of agricultural materials. The authors found that optimising the geometric parameters of the screw and the operating mode can significantly reduce energy consumption and increase transport productivity. This is especially relevant for systems that work with bulk materials, where it is important to avoid clogging and wear of equipment. W. Yu *et al.* (2022) simulated the transportation of concrete by a screw conveyor using the discrete element method. The authors analysed the influence of the screw angle, rotation speed and material properties on transportation efficiency. The study showed that incorrect selection of screw surface parameters can lead to component segregation or increased energy consumption. The results of this study are

important for construction and building materials production, where dosing accuracy and mixture homogeneity are critical.

Scientists T. Lahari *et al.* (2022) analysed the parameters of a single-screw extruder for plastic processing. The authors studied the influence of temperature, screw rotation speed and channel geometry on the quality of the extruded material. The study showed that optimising these parameters improves melt homogeneity and reduces defects in the final product. T. Senfter *et al.* (2024) investigated the effectiveness of a screw press for atypical substrates such as manure and organic waste. They found that the performance of the press depends significantly on the moisture content and composition of the substrate, as well as on the design features of the press, in particular the angle of the screw and the size of the filter holes. The study emphasised the importance of adapting equipment to specific operating conditions, which is particularly relevant for agriculture and bioenergy. Similar results regarding the effectiveness of using screw elements to optimise energy consumption were obtained in a study by H. Parlamış *et al.* (2021), which conducted an experimental analysis of a solar air collector with a screw insert. This highlights the versatility of screw surfaces as an energy-saving solution in various industries.

Researchers S. Fu *et al.* (2023) analysed the factors that influence the efficiency of separation by screw presses, in particular for the treatment of suspensions and slurries. The authors found that the key parameters are screw rotation speed, outlet pressure, and solid phase content in the suspension. The authors proposed a mathematical model that allows predicting the press performance based on these parameters, which is important for optimising dewatering processes in industry. D. Mondal (2020a; 2020b) presented a methodological approach to the design of an experimental laboratory screw conveyor, taking into account two types of working surface coating. The author compared the productivity of conveyors with smooth and corrugated coatings and demonstrated that corrugated coatings reduce material slippage and increase transport efficiency. The study also included an analysis of the effect of the conveyor angle on its productivity, which is important for the design of transport systems in confined spaces.

S. Mirzaei & L. Shen (2021) optimised water utilisation in a screw press for paper production. The study investigated the effect of pressure, screw rotation speed and fibre concentration on the efficiency of pulp dewatering. The study showed that optimal parameters can reduce energy consumption and improve the quality of pressing, which is important for the paper industry. V. Bulgakov *et al.* (2022) studied the dynamic loads on a sectional flexible screw conveyor during the transportation of agricultural materials. They found that uneven loading and vibrations can lead to premature equipment wear, so they proposed methods to reduce dynamic loads by optimising the conveyor design. S. Moorthi *et al.* (2022) conducted a dynamic analysis of a single-screw conveyor for specific industrial needs, in particular for transporting abrasive materials. The authors investigated the effect of rotation speed, angle of inclination, and screw material on vibration levels and energy consumption. The study showed that optimising these parameters reduces equipment wear and improves performance. Z. Chen *et al.* (2024) investigated the effect of bone density on the screw's ability to fix in orthopaedic surgery. The authors found that the optimal screw design and material selection depend on local bone density, which is particularly important for ensuring implant stability.

The aim of the work was to analytically describe the movement of a load along a screw surface, given by the curve of its axial cross-section in the form of a parabola, under the action of its own weight, using the example of a material particle. The objectives of the study were to compile differential equations of particle sliding, solve them using numerical methods, and find dependencies between particle sliding parameters and the shape of the curve after movement stabilisation.

Materials and Methods

The research methods were based on the principles of mechanics and differential geometry of surfaces. Numerical integration was performed using the Simulink dynamic modelling package of the MatLab software product. The differential equation of particle motion in vector form was as follows: $m\bar{w} = \bar{F}$, where m – the mass of the particle, $\bar{w}$ – the acceleration vector, $\bar{F}$ – the total vector of forces applied to the particle. The simplest case is the free fall of a particle, in which the applied force was the force of its own weight, as well as the force of air resistance. If the particle moved along the surface, then there was also a reaction force and a friction force dependent on it. The force of gravity was directed downwards, the reaction force was normal to the surface, and the friction and air resistance forces were in the opposite direction to the particle's velocity. The friction force F_f (Fig. 1b) was the product of the friction coefficient f and the reaction force R: $F_f = fR$.

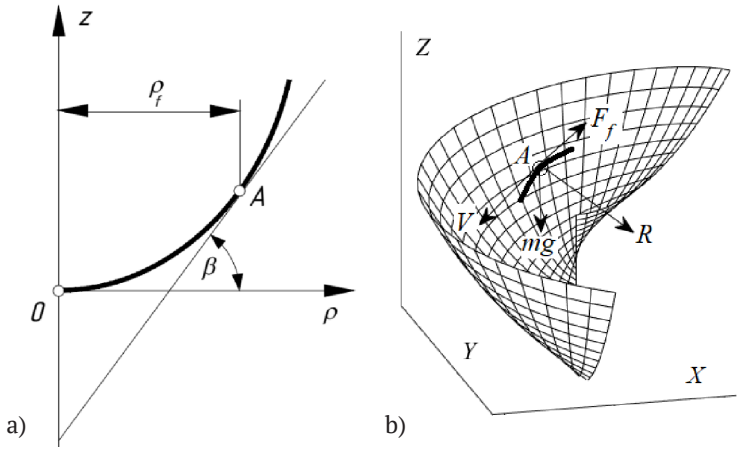

Figure 1. *Graphic illustrations of the formation of a helical surface*

Note: a) curve of the axial cross-section of the helical surface; b) helical surface formed by a combination of rotational and translational movements along the axis; 0z, 0ρ, X, Y, Z – coordinate axes, units of measurement– m; A – current point on the surface; β – angle of inclination of the tangent to the curve of the axial cross-section of the surface at the current point to the horizontal plane of projections; V – direction of the particle's sliding velocity vector; mg – weight force; R – surface reaction; Ff –friction force vector

Source: developed by the authors

Air resistance was neglected because it is insignificant at low speeds. The differential equations of motion of a point on a surface in projections onto a stationary coordinate system had the form:

$$\begin{aligned} mx'' &= -fRT_x + RN_x; \\ my'' &= -fRT_y + RN_y; \\ mz'' &= -fRT_z + RN_{z-mg}, \end{aligned} \qquad (1)$$

where R – surface reaction force; T_x, T_y, T_z – projections of the unit vector tangent to the trajectory; N_x, N_y, N_z – projections of the unit vector normal to the surface along the trajectory, x'', y'', z'' – projections of particle acceleration. The surface was defined by parametric equations in terms of two independent variables ρ and α: $X = X(\rho, \alpha)$, $Y = Y(\rho, \alpha)$, $Z = Z(\rho, \alpha)$. The variables ρ and α were dependent on time t: $\rho = \rho(t)$ and $\alpha = \alpha(t)$. In this case, the surface equation was transformed into the equation of a line on it. This line was the sought-after trajectory, which became known when the dependencies $\rho = \rho(t)$ and $\alpha = \alpha(t)$ were found after solving the system of equations (1).

Results

The curve of the axial cross-section of the surface is given by the equation in explicit form: $z = z(\rho)$ (Fig. 1a). If such a curve is rotated around the z-axis, a surface of revolution is formed. In addition to the rotational motion, the curve is given a translational motion along the z-axis, and the relationship between the angle of rotation α and the translational motion is linear: $z = b\alpha$ (Fig. 1b). The constant b is a screw parameter. In this case, the parametric equations of the surface are written as:

$$\begin{aligned} X &= \rho\cos\alpha; \\ Y &= \rho\sin\alpha; \\ Z &= z(\rho) - b\alpha. \end{aligned} \qquad (2)$$

The sign '–' in the last equation (2) means that when the curve rotates around the z-axis, it simultaneously moves downwards. Then the tangent to the trajectory will also be directed in accordance with the movement of the particle along the surface, i.e. towards its descent. With the dependencies $\rho = \rho(t)$ and $\alpha = \alpha(t)$ established, the surface equations (2) are transformed into the equations of the line on it. To distinguish between the surface equations and the analogous line equations on it, the coordinates of the surface points are denoted by capital letters "X", "Y", "Z", and the coordinates of the line points on the surface are denoted by lowercase letters "x", "y", "z". The projections of the particle's sliding velocity are found by differentiating equations (2), taking into account that $\rho = \rho(t)$ and $\alpha = \alpha(t)$. In this case, the derivative $z(\rho)$ with respect to the variable ρ is denoted by the corresponding subscript, and the derivatives with respect to time t are denoted without an index:

$$\begin{aligned} x' &= \rho'\cos\alpha - \rho\alpha'\sin\alpha; \\ y' &= \rho'\sin\alpha + \rho\alpha'\cos\alpha; \\ z' &= z_\rho'\rho' - b\alpha'. \end{aligned} \qquad (3)$$

The magnitude of the particle's sliding velocity is the vector sum of the projections (3):

$$V = \sqrt{x'^2 + y'^2 + z'^2} = \\ = \sqrt{\alpha'^2(\rho^2 + b^2) - 2b\rho'\alpha' z_\rho' + \rho'^2\left(1 + z_\rho'^2\right)}. \qquad (4)$$

The projections T_x, T_y, T_z of the unit vector tangent to the trajectory can be found by dividing the corresponding projections (3) by the velocity (4):

$$T_x = \frac{\rho'\cos\alpha - \rho\alpha'\sin\alpha}{\sqrt{\alpha'^2(\rho^2+b^2) - 2b\rho'\alpha' z_\rho' + \rho'^2\left(1+z_\rho'^2\right)}}; \\ T_y = \frac{\rho'\sin\alpha + \rho\alpha'\cos\alpha}{\sqrt{\alpha'^2(\rho^2+b^2) - 2b\rho'\alpha' z_\rho' + \rho'^2\left(1+z_\rho'^2\right)}}; \\ T_z = \frac{z_\rho'\rho' - b\alpha'}{\sqrt{\alpha'^2(\rho^2+b^2) - 2b\rho'\alpha' z_\rho' + \rho'^2\left(1+z_\rho'^2\right)}}. \qquad (5)$$

By differentiating expressions (3), the second derivatives of the trajectory equations can be obtained, i.e. the projections of acceleration:

$$\begin{aligned} x'' &= (\rho'' - \rho\alpha'^2)\cos\alpha - (\rho\alpha'' + 2\rho'\alpha')\sin\alpha; \\ y'' &= (\rho'' - \rho\alpha'^2)\sin\alpha + (\rho\alpha'' + 2\rho'\alpha')\cos\alpha; \\ z'' &= z_\rho''\rho'^2 + z_\rho'\rho'' - b\alpha''. \end{aligned} \qquad (6)$$

The coordinates of the vector $\bar{N}$ normal to the surface are defined as the vector product of two vectors tangent to the coordinate lines. The projections of these vectors are the first-order partial derivatives of the surface (2):

$$\begin{aligned} X_\rho' &= \cos\alpha;\ Y_\rho' = \sin\alpha;\ Z_\rho' = z_\rho'; \\ X_\alpha' &= -\rho\sin\alpha;\ Y_\alpha' = \rho\cos\alpha;\ Z_\alpha' = -b. \end{aligned} \qquad (7)$$

In derivatives (7), the lower index denotes the variable by which differentiation occurs. The vector product of vectors (7) is written as:

$$\bar{N} = \begin{vmatrix} X & Y & Z \\ X_\alpha' & Y_\alpha' & Z_\alpha' \\ X_\rho' & Y_\rho' & X_\rho' \end{vmatrix} = \begin{Bmatrix} -b\sin\alpha - \rho z_\rho'\cos\alpha; \\ b\cos\alpha - \rho z_\rho'\sin\alpha; \\ \rho. \end{Bmatrix}. \qquad (8)$$

The normal vector (8) must be reduced to unity. After that, its projections N_x, N_y, N_z will be written as:

$$N_x = -\frac{b\sin\alpha + \rho z_\rho'\cos\alpha}{\sqrt{\rho^2\left(1+z_\rho'^2\right)+b^2}}; \\ N_y = \frac{b\cos\alpha - \rho z_\rho'\sin\alpha}{\sqrt{\rho^2\left(1+z_\rho'^2\right)+b^2}}; \\ N_z = \frac{\rho}{\sqrt{\rho^2\left(1+z_\rho'^2\right)+b^2}}. \qquad (9)$$

It should be noted that the direction of the normal vector can be directed in one or the opposite direction from the surface. This depends on the order of the vectors (7) in the determinant (8). It is necessary to ensure that it coincides with the direction of the reaction force R (Fig. 1b). Since the particle presses down on the surface, the reaction of the surface will be directed upwards. This means that the expression N_z in (9) must be positive. Taking into account expressions (5) and (9), system (1) takes the form:

$$mx'' = -fR\frac{\rho'\cos\alpha-\rho\alpha'\sin\alpha}{\sqrt{\alpha'^2(\rho^2+b^2)-2b\rho'\alpha'z'_\rho+\rho'^2\left(1+z'^2_\rho\right)}} - R\frac{b\sin\alpha+\rho z'_\rho\cos\alpha}{\sqrt{\rho^2\left(1+z'^2_\rho\right)+b^2}};$$

$$my'' = -fR\frac{\rho'\sin\alpha+\rho\alpha'\cos\alpha}{\sqrt{\alpha'^2(\rho^2+b^2)-2b\rho'\alpha'z'_\rho+\rho'^2\left(1+z'^2_\rho\right)}} + R\frac{b\cos\alpha-\rho z'_\rho\sin\alpha}{\sqrt{\rho^2\left(1+z'^2_\rho\right)+b^2}};$$

$$mz'' = -fR\frac{z'_\rho\rho'-b\alpha'}{\sqrt{\alpha'^2(\rho^2+b^2)-2b\rho'\alpha'z'_\rho+\rho'^2\left(1+z'^2_\rho\right)}} + R\frac{\rho}{\sqrt{\rho^2\left(1+z'^2_\rho\right)+b^2}} - mg. \quad (10)$$

Substituting the acceleration projections from (6) into (10) gives a system of three differential equations with unknown dependencies $\rho=\rho(t)$, $\alpha=\alpha(t)$ amd $R=R(t)$. The resulting system must be solved with respect to the second derivatives ρ'', α'' and the reaction force R, since this notation allows for numerical integration of the system. After that, system (10) takes the form:

$$\alpha'' = \frac{b\left(g+\alpha'^2\rho z'_\rho+\rho'^2z''_\rho\right)-2\alpha'\rho'\rho\left(1+z'^2_\rho\right)}{A^2} - \frac{f\alpha'B}{AV};$$

$$\rho'' = \rho\frac{b^2\alpha'^2-2b\alpha'\rho'z'_\rho+\rho[\alpha'^2\rho-z'_\rho(g+\rho'^2z''_\rho)]}{A^2} - \frac{f\rho'B}{AV};$$

$$R = \frac{mB}{A}, \quad (11)$$

where A, B, V denote repeated expressions. Among them is the velocity V, the expression for which is given in (4), as well as others, which have the following form: $A=\sqrt{\rho^2\left(1+z'^2_\rho\right)+b^2}$, $B=\rho g+\alpha'^2\rho^2 z'_\rho+2b\alpha'\rho'+\rho\rho'^2z''_\rho$.

When a particle slides along a screw surface with a constant pitch, its motion stabilises after a transition period. The particle moves at a constant speed V, its angular velocity of rotation around the surface axis $\alpha'=\omega$ is also constant, and the distance ρ from the surface axis is also constant. It follows that: $\alpha''=0, \rho''=\rho'=0$. Substituting these values of the variables into the first equation of system (11) gives the result:

$$0 = \frac{(bV-f\alpha'\rho A)(g+\alpha'^2\rho z'_\rho)}{AV}. \quad (12)$$

In equation (12), only one expression in brackets can be equal to zero with a difference in terms. Its solution with respect to b is as follows:

$$b = \frac{\rho}{\sqrt{2}}\sqrt{f^2-1+\sqrt{1+f^4+2f^2\left(1+2z'^2_\rho\right)}}. \quad (13)$$

Equation (13) shows that the distance ρ from the axis to the particle's sliding trajectory after stabilisation of motion depends on the friction coefficient f and the derivative of the curve equation $z=z(\rho)$ with respect to the variable ρ. But this derivative is equal to the tangent of the angle β of inclination of the tangent to the curve: $z'_\rho=tg\beta$ At a given angle β and a known friction coefficient f, the motion of a particle along a screw surface will be analogous to the motion along a helicoid formed by a set of straight generatrices inclined at an angle β. In other words, the curve of the axial cross-section of the helicoid will be a straight line inclined at an angle β. With a known coefficient f, the distance of the particle's sliding along the helicoid from its axis is uniquely determined (in Fig. 1a, it is marked ρ_f). With a curved cross-section, this distance is also uniquely determined, but when the coefficient f changes, the distance ρ_f for the helicoid and the helical surface will be different. In addition, using the constant (constants) included in the equation $z=z(\rho)$ it is possible to change the shape of the curve.

Substituting into the second equation of system (11) $\rho'' = \rho' = 0$ gives the expression:

$$0 = \alpha'^2 (\rho^2 + b^2) - g\rho z'_\rho. \quad (14)$$

From (14), an angular velocity $\alpha' = \omega$ can be determined for the rotation of a particle around the axis of the screw surface:

$$\alpha' = \omega = \sqrt{\frac{\rho g z'_\rho}{\rho^2 + b^2}}. \quad (15)$$

From expression (4), substituting it into (15) at $\rho' = 0$, the sliding velocity of the particle can be found:

$$V = \sqrt{\rho g z'_\rho}. \quad (16)$$

The dependencies obtained (13), (15) and (16) are sufficient for calculating the screw pitch. Here is an example. The curve of the axial cross-section of the screw surface is taken to be a parabola $z = a\rho^2$. Thus $z'_\rho = 2a\rho$, $z''_\rho = 2a$. According to (16):

$$V = \rho\sqrt{2ag}, \text{ from } a = \frac{V^2}{\sqrt{2g\rho^2}}. \quad (17)$$

Thanks to the constant a, it is possible to set the desired sliding speed V of the particle at a given distance ρ from the surface axis. To ensure high-quality performance of the technological process, the speed must be limited. Let $V = 2$ *m/s*, $\rho = 0.4$ *m*. From the second expression (17): $a = 1.27$. From expression (13), with a known coefficient $f = 0.3$, the screw parameter b can be found: $b = 0.16$. Two constants a and b are sufficient to construct the surface according to equations (2). The surface with the particle's motion trajectories plotted is shown in Figure 2a. The trajectories of the particle after stabilisation are shown by thick lines for the corresponding friction coefficient f. The value ρ = 0.4 m corresponds to the friction coefficient $f = 0.3$. For a particle with a different friction coefficient, for example, $f = 0.2$, the trajectory will be different for this surface. Finding it using the obtained dependencies is difficult and involves cumbersome expressions and numerical calculations. However, the trajectory can be constructed using numerical integration of system (11). In Figure 2b, the dashed line shows the trajectory of a particle that is fed onto the surface at zero velocity at a distance of *0.1 m* from its axis.

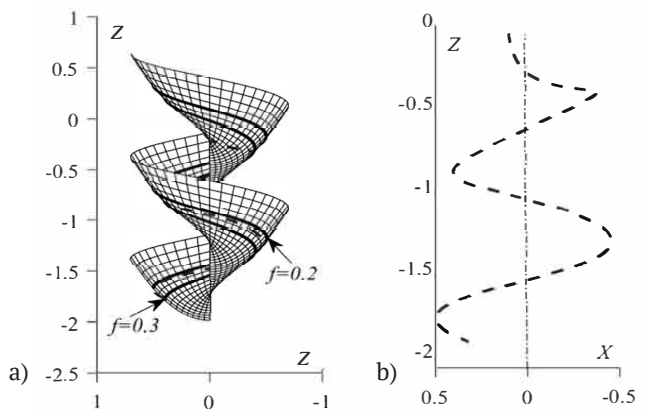

Figure 2. *Graphical illustrations of particle motion on a surface*
Note: a) frontal projection of the surface with motion trajectories marked; b) particle motion trajectory during acceleration; X, Z – coordinate axes, units of measurement – m, f – friction coefficient
Source: developed by the authors

From the analysis of Figure 2b, it can be concluded that the distance ρ increases as the particle slides. This is clearly demonstrated by the graph of the change in distance ρ over 4

seconds from the start of movement (Fig. 3a). It shows that as the motion stabilises, the distance approaches a steady value of $\rho = 0.5$ *m*. Substituting $f = 0.2$ and $\rho = 0.5$ m into expression (13) gives the result: $b = 0.16$, i.e. the value of the screw parameter for which this surface is constructed. In Figure 2a, for $f = 0.2$, the trajectory after stabilisation of motion and the trajectory of motion are plotted as a dashed line during the transition period (in Figure 2a, it is plotted separately).

Figure 3b shows that as the motion stabilises, the particle velocity approaches a value of $V = 2.5$ *m/s*. From the first formula (17) with $\rho = 0{,}5$ *m* and the previous value of a $a = 1.27$ the same velocity value is calculated.

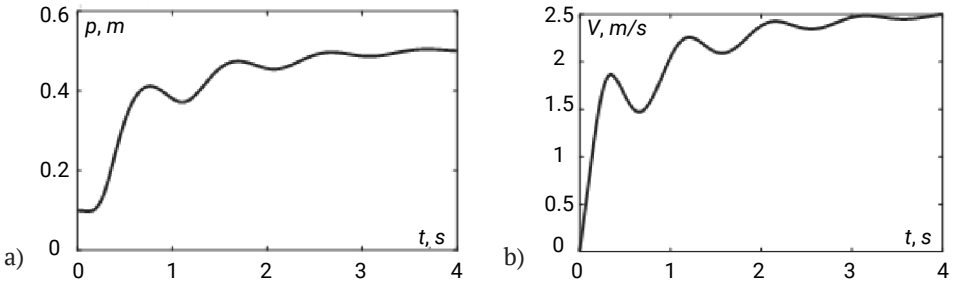

Figure 3. *Graphs of the kinematic parameters of the particle in the transition period*
Note: a) graph of the change in the distance ρ of the trajectory from the surface axis; b) graph of the change in the sliding velocity V; ρ – current distance of the particle from the axis of the helical surface during sliding; V – sliding velocity; t – time
Source: developed by the authors

Discussion

It is advisable to compare the results obtained with those obtained by T.A. Kresan (2020). The author describes that the helical surface is formed by a set of straight generatrices inclined at a constant angle to the horizontal plane, i.e. it is an oblique closed helicoid. The axial cross-section is a straight line that cannot change its shape. T.A. Kresan noted that when the straight generatrices of the helicoid are inclined at $\beta = 30°$ and the screw parameter is $b = 0.24$ (these two parameters define the helicoid), a particle with a friction coefficient $f = 0.3$ slides along the surface at a speed $V = 2$ *m/s* at a distance $\rho = 0.7$ *m*. The results presented in the work of T.A. Kresan (2020) can be obtained in the presented study as a special case. To do this, it is necessary to find the value of the constant a that corresponds to the angle $\beta = 30°$ and $\rho = 0.7$ m. Based on the fact that $z'_\rho = \mathrm{tg}\beta = 0.577$, i.e. for the parabola $2a\rho = 0.577$, it is determined that: $a = 0.41$. Using formula (13), the screw parameter b can be obtained at $f = 0.3$ and $\rho = 0.7$ m: $b = 0.24$. Using the first formula (17), the sliding velocity of the particle at $\rho = 0.7$ m and $a = 0.41$ can be determined: *m/s*. Thus, the results obtained fully coincide with the results obtained by T.A. Kresan (2020), which are a special case of the presented study. Due to the curved axial cross-section of the helical surface in the form of a parabola, it is possible to change the constant a so that the velocity remains the same ($V = 2$ *m/s*), but the distance ρ is different (for example, $\rho = 0.2$ *m* as opposed to $\rho = 0.4$ *m* in the previous case). Then, according to the second expression (17), $a = 4.5$. When the shape of the parabola changes, the screw parameter b also changes. It can be found using the formula (13): $b = 0.11$. In this case, the particle's descent speed will be higher, since at a constant speed $V = 2$ *m/s*, the sliding path has decreased due to the reduction in distance ρ and pitch b.

Other scientists, M. Gamtsemlidze *et al.* (2024), investigated the optimal parameters of a screw separator for coal slurry enrichment,

focusing on the influence of the axial cross-section shape on separation efficiency. They showed that curved cross-sections (e.g., elliptical) improve particle distribution by density compared to straight ones. The present study confirms these findings: it also demonstrates that a curved cross-section (parabola) provides greater flexibility in controlling the trajectory and velocity of particles. However, unlike M. Gamtsemlidze *et al.* (2024), who focused on separation properties, this study focuses on the analytical description of motion and the optimisation of kinematic parameters, which expands the possibilities for designing screw chutes for transportation. V. Hud *et al.* (2023) proposed a multifunctional screw conveyor separator for agricultural materials, where the key was to analyse the effect of screw geometry on separation efficiency. They found that variable screw geometry (e.g., variable pitch) can increase productivity by 15-20%. The current study complements these results: it shows that even with a fixed pitch but a curved cross-section, a similar effect can be achieved by changing the shape of the curve (e.g., a parabola). This is especially important for systems where changing the pitch is technically difficult. It is worth noting that similar approaches to optimising mineral processing are also demonstrated by recent studies on the extraction of rare elements. For example, J. Corchado-Albelo & L. Alagha (2024) showed that the mineralogical characteristics of copper tailings determine the efficiency of tellurium extraction, which is consistent with the idea of adapting the design of screw surfaces to the properties of the source material.

O. Lyashuk *et al.* (2019) developed a mathematical model for transporting bulk materials using a tubular screw conveyor, focusing on the impact of the conveyor angle and friction coefficient on productivity. They showed that the optimal angle depends on the properties of the material. The present study extends this approach: not only is the angle of inclination taken into account (via $tg\beta$ in the curve equation), but it is also demonstrated how the cross-sectional shape (parabola) affects the stabilisation of particle motion. This allows for more accurate design of systems for materials with different rheological properties. Y. Indartono *et al.* (2019) and O. Fakayode *et al.* (2019) devoted their work to optimising screw presses for extracting oil from plant raw materials. Y. Indartono *et al.* (2019) investigated the influence of screw geometry on the efficiency of oil extraction from calophyllum seeds, while O. Fakayode *et al.* (2019) optimised the parameters of the press for moringa seeds. Both studies emphasise that the optimal screw geometry depends on the moisture content and particle size of the raw material. The present study complements these findings by showing that for materials with different friction coefficients (which depend on moisture content), a curved cross-section shape can be selected to ensure a stable sliding speed. This is particularly relevant for presses, where it is important to avoid clogging or uneven material movement.

Researchers B. El Idrissi *et al.* (2020) and T. Eaves *et al.* (2020) simulated the process of wood pulp dewatering in screw presses, focusing on the effect of pressure and moisture on productivity. The authors showed that the optimal pressure depends on the content of fine fibres in the suspension. T. Eaves *et al.* (2020) investigated the dewatering of saturated suspensions, emphasising the role of the rheological properties of the material. The current study extends these findings: for materials with different rheological characteristics (which affect the friction coefficient f), an appropriate cross-sectional curve shape can be selected to optimise the speed and trajectory of movement. This is particularly important for presses, where uniform dewatering must be ensured without loss of productivity. E. Loranger *et al.* (2019) investigated the effect of dewatering parameters (rotation speed, pressure) on the performance of a screw press for pulp. They showed that the optimal parameters depend on the concentration of fibres and their length. The present study complements these results: it shows that the shape of the curved cross-section (e.g. parabola) allows

additional control of the kinematic parameters, which is particularly important for materials with unstable properties (e.g. variable moisture content).

P.G. Chitte *et al*. (2022) developed a methodology for designing a screw press for dewatering, focusing on the influence of filter hole geometry and screw angle. The authors showed that the optimal geometry depends on the properties of the slurry. The present study extends this approach: the shape of the axial cross-section (parabola) can also be used as an optimisation tool, especially for materials that are difficult to dewater due to their high content of fine particles. B. El Idrissi *et al*. (2019) investigated the parameters of wood pulp dewatering in a screw press, focusing on the influence of operating parameters – such as screw rotation speed, outlet pressure and pulp properties (in particular, fine fibre content and moisture content) – on process efficiency. The authors showed that the optimal dewatering conditions depend on the rheological characteristics of the material: for example, for pulp with a high content of fine fibres, it is necessary to increase the outlet pressure to achieve the desired dryness of the press cake. They also emphasised that the screw rotation speed must be adapted to the viscosity of the pulp to avoid excessive energy consumption or uneven dewatering. The presented study complements these findings by proposing an analytical approach to controlling the kinematic parameters of particle movement on screw surfaces. While B. El Idrissi *et al*. (2019) focused on experimentally determining the optimal parameters for specific types of pulp, the present study shows how the shape of the curved axial cross-section (e.g., a parabola) can be used to more precisely control the trajectory and speed of particle movement. For example, the paper demonstrates that by changing the constant a in the parabolic curve equation $z = a\rho^2$ it is possible to ensure a stable particle sliding speed even when the friction coefficient f, which depends on the moisture content and composition of the material, changes. This allows screw surfaces to be adapted to different types of pulp without the need to change the screw design, which is an important advantage for industrial applications where material properties may vary. Thus, the presented study extends the results of B. El Idrissi *et al*. (2019), offering an analytical tool for optimising screw surfaces, taking into account not only operating parameters but also the geometry of the axial cross-section, which opens up new opportunities for improving dewatering efficiency.

The study made it possible to build an analytical model of particle motion along a screw surface with a curved axial cross-section and to verify its adequacy using a parabola as an example. The obtained dependencies allow determining the sliding speed and the distance of the particle from the surface axis after stabilisation of motion, as well as selecting the necessary surface parameters for the given operating conditions. The proposed approach expands the possibilities of controlling the kinematic characteristics of motion compared to classical models for an oblique helicoid and provides a more accurate calculation of helical descents. The results obtained allow not only to analytically describe the motion of a particle along a helical surface with a curved axial cross-section, but also to optimise the kinematic parameters for specific technological conditions.

Conclusions

A screw chute can be formed by anoblique helicoid with a straight line as its axial cross-section, as well as by a non-linear helical surface with a curved axial cross-section. Differential equations of motion of a particle along a helical surface with a curved cross-section, the shape of which is given by an explicit equation, have been derived. Using a parabola as an example of an axial cross-section, the differential equations were numerically integrated and the patterns of change in kinematic parameters during the transition period were obtained. Formulas were derived that relate the shape of the axial cross-section curve (given by the equation $z = a\rho^2$ for a parabola) to the kinematic parameters of the particle – the

sliding velocity V and the distance from the axis ρ. For example, for a parabolic shape with a constant $a = 1.27$ and a distance $\rho = 0.4$ m, a sliding velocity $V = 2$ *m/s* was obtained, which meets the requirements of many industrial applications. Analytical dependencies were derived that give numerical values of these parameters after the particle's motion stabilises. Using numerical integration of a system of differential equations, it was shown that after a transition period (about 3-4 seconds), the particle moves at a constant speed and distance from the axis. For example, for a particle with a friction coefficient $f = 0.2$, which is fed to the surface with zero velocity at a distance of *0.1 m* from the axis, the velocity stabilises at $V = 2.5$ *m/s*, and the distance ρ approaches *0.5 m*. It is shown that the curved axial cross-section of the helical surface provides broader opportunities for controlling the kinematic parameters of particle motion compared to a straight cross-section. In the article, this is demonstrated by comparing the known results of particle motion along an oblique helicoid, which is a special case of the studies presented, with the results obtained. It is shown that at a friction coefficient $f = 0.3$ and a distance $\rho = 0.7$ m, the screw parameter is $b = 0.24$, which completely coincides with the results of previous studies for a straight cross-section. However, with a curved cross-section, it is possible to change the constant a so as to maintain a speed of $V = 2$ *m/s* at a different distance ρ. This indicates greater flexibility in the design of helical descents.

During the study, an analytical model of the motion of a material particle along a screw surface with a curved axial cross-section was developed, which allows optimising the kinematic parameters for specific technological conditions. Unlike traditional approaches, where screw surfaces are considered as oblique helicoids with a straight axial cross-section, it has been shown that the use of curved cross-sections significantly expands the possibilities for controlling particle motion. Prospects for further research lie in the experimental verification of the obtained analytical dependencies for real materials and in the extension of the model to the case of a variable friction coefficient.

Acknowledgements

The authors of the article express their gratitude to the soldiers of the Armed Forces of Ukraine, whose bravery allows the scientists of Ukraine to continue their research.

Funding

None.

Conflict of Interest

None.

References

[1] Bulgakov, V., Pascuzzi, S., Adamchuck, V., Olt, J., Ruzhylo, Z., Trokhnaniak, O., Santoro, F., Arak, M., Nowak, J., & Beloev, H. (2023). Research into power and load parameters of flexible screw conveyors for transportation of agricultural materials. In *Farm machinery and processes management in sustainable agriculture* (vol. 289, pp. 61-75). Cham: Springer International Publishing. doi: 10.1007/978-3-031-13090-8_6.

[2] Bulgakov, V., Trokhnaniak, O., Adamchuck, V., Chernovol, M., Korenko, M., Dukulis, I., & Ivanovs, S. (2022). A study of dynamic loads of a flexible sectional screw conveyor. *Acta Technologica Agriculturae*, 25(3), 131-136. doi: 10.2478/ata-2022-0020.

[3] Chen, Z., Chen, Y., Zhou, J., He, Y., & Li, J. (2024). The bony density of the pedicle plays a more significant role in the screw anchorage ability than other regions of the screw trajectory. *Orthopaedic Surgery*. doi: 10.1111/os.14299.

[4] Chitte, P.G., Tapsi, P., & Deshmukh, B. (2022). Design and development of dewatering screw press. In *Recent advances in manufacturing modelling and optimization* (pp. 569-578). Singapore: Springer. doi: 10.1007/978-981-16-9952-8_48.

[5] Corchado-Albelo, J., & Alagha, L. (2024). Tellurium enrichment in copper tailings: A mineralogical and processing study. *Minerals*, 14(8), article number 761. doi: 10.3390/min14080761.

[6] Eaves, T.S., Paterson, D.T., Hewitt, D.R., Balmforth, N.J., & Martinez, D.M. (2020). Dewatering saturated, networked suspensions with a screw press. *Journal of Engineering Mathematics*, 120, 1-28. doi: 10.1007/s10665-019-10029-3.

[7] El Idrissi, B., Loranger, É., & Lanouette, R. (2020). Modelling of dewatering wood pulp in a screw press using statistical and multivariate analysis. *BioResources*, 15, 5899-5912. doi: 10.15376/biores.15.3.5899-5912.

[8] El Idrissi, B., Loranger, É., Lanouette, R., Bousquet, J.P., & Martinez, M. (2019). Dewatering parameters in a screw press and their influence on the screw press outputs. *Chemical Engineering Research and Design*, 152, 300-308. doi: 10.1016/j.cherd.2019.10.001.

[9] Fakayode, O.A., & Ajav, E.A. (2019). Development, testing and optimization of a screw press oil expeller for moringa (Moringa oleifera) seeds. *Agricultural Research*, 8, 102-115. doi: 10.1007/s40003-018-0342-6.

[10] Fu, S., Dou, B., Zhang, X., & Li, K. (2023). An interactive analysis of influencing factors on the separation performance of the screw press. *Separations*, 10, article number 245. doi: 10.3390/separations10040245.

[11] Gamtsemlidze, M., Enageli, R., & Oniani, M. (2024). Evaluation of the optimal parameters of the coal silt enrichment process on the screw like separator. *Works of Georgian Technical University*, 1(531), 267-275. doi: 10.36073/1512-0996-2024-1-267-275

[12] Hud, V., Lyashuk, O., Hevko, I., Ungureanu, N., Vlăduț, N.-V., Stashkiv, M., Hevko, O., & Pik, A. (2023). Enhancement of agricultural materials separation efficiency using a multi-purpose screw conveyor-separator. *Agriculture*, 13(4), article number 870. doi: 10.3390/agriculture13040870.

[13] Indartono, Y.S., Heriawan, H., & Kartika, I.A. (2019). Innovative and flexible single screw press for the oil extraction of Calophyllum seeds. *Research in Agricultural Engineering*, 65, 91-97. doi: 10.17221/85/2018-RAE.

[14] Kresan, T.A. (2020). Calculation of gravitation descent formed by surface of skew closed helicoid. *Machinery & Energetics*, 11(2), 49-57.

[15] Lahari, T.R., & Srinivas Sharma, G. (2022). Parametric analysis of single screw extruder for processing of re-cycled plastics. *International Journal of Current Engineering and Technology*, 12(1), 9-14.

[16] Lyashuk, O., Vovk, Y., Sokil, B., Klendii, V., Ivasechko, R., & Dovbush, T. (2019). Mathematical model of a dynamic process of transporting a bulk material by means of a tube scraping conveyor. *Agricultural Engineering International: CIGR Journal*, 21(1), 74-81.

[17] Mirzaei, S., & Shen, L. (2021). Water disposal minimization of a screw press in the tissue manufacturing process. *The International Journal of Advanced Manufacturing Technology*, 115, 2659-2667. doi: 10.1007/s00170-021-07247-4.

[18] Mondal, D. (2020a). A short spiral conveyor using cut flight screw with two different trough cover of different height – a comparative study. In *Techno-societal 2020* (pp. 695-703). Cham: Springer. doi: 10.1007/978-3-030-69925-3_67.

[19] Mondal, D. (2020b). Design consideration of a laboratory size screw conveyor with variable speed for experimentation purpose – a methodological approach. In *Techno-societal 2020* (pp. 705-714). Cham: Springer. doi: 10.1007/978-3-030-69925-3_68.

[20] Moorthi, S., Megaraj, M., Nagarajan, L., Karthick, A., Bharani, M., & Patil, P.P. (2022). Dynamic analysis and fabrication of single screw conveyor machine. *Advances in Material Science and Engineering*, 10, article number 812754. doi: 10.1155/2022/3843968.

[21] Parlamış, H., Özden, E., & Büker, M.S. (2021). Experimental performance analysis of a parabolic trough solar air collector with helical-screw tape insert: A comparative study. *Sustainable Energy Technologies and Assessments*, 47(3), article number 101562. doi: 10.1016/j.seta.2021.101562.

[22] Senfter, T., Schweiggl, I., Berger, M., Mayerl, C., Kofler, T., Kraxner, M., Steffens, A., & Pillei, M. (2024). The dewatering performance of a compact screw press manure separator for non-typical substrates. *Separations*, 11(1), article number 28. doi: 10.3390/separations11010028.

[23] Yu, W., Zhang, K., Li, D., Zou, D., & Zhang, S. (2022). Numerical modeling of concrete conveying capacity of screw conveyor based on DEM. *Powder Technology*, 29, 361-374. doi: 10.12989/cac.2022.29.6.361.

Розрахунок гравітаційного гвинтового спуску, у якого крива осьового перерізу задана явним рівнянням

Сергій Пилипака
Доктор технічних наук, професор
Національний університет біоресурсів і природокористування України
03041, вул. Героїв Оборони, 15, м. Київ, Україна
https://orcid.org/0000-0002-1496-4615
Тетяна Воліна
Доктор технічних наук, доцент
Національний університет біоресурсів і природокористування України
03041, вул. Героїв Оборони, 15, м. Київ, Україна
https://orcid.org/0000-0001-8610-2208
Віктор Несвідомін
Доктор технічних наук, професор
Національний університет біоресурсів і природокористування України
03041, вул. Героїв Оборони, 15, м. Київ, Україна
https://orcid.org/0000-0002-1495-1718
Віталій Бабка
Кандидат технічних наук, доцент
Національний університет біоресурсів і природокористування України
03041, вул. Героїв Оборони, 15, м. Київ, Україна
https://orcid.org/0000-0003-4971-4285
Тарас Пилипака
Кандидат технічних наук, доцент
Національний університет водного господарства та природокористування
33028, вул. Соборна, 11, м. Рівне, Україна
https://orcid.org/0009-0000-5582-1859

Анотація. Гвинтові гравітаційні спуски використовуються для безенергетичного транспортування вантажів і гравітаційної сепарації руд, що зумовлює необхідність оптимального поєднання конструктивних параметрів робочої поверхні, швидкості руху та компактності траєкторії. Метою роботи був аналітичний опис руху вантажу по гвинтовій поверхні, заданій кривою її осьового перерізу, під дією сили власної ваги на прикладі матеріальної частинки. Для розв'язання було використано методи класичної механіки, диференціальної теорії поверхонь і чисельні методи. Основні результати дослідження ґрунтувались на тому, що після стабілізації руху матеріальна частинка починає ковзати по поверхні зі сталою швидкістю і сталою відстанню від осі гвинтової поверхні з урахуванням форми кривої її осьового перерізу. Встановлено, що до рівняння цієї кривої можуть входити сталі величини, які впливають на її форму, тобто на кінематичні параметри частинки. Це дало можливість знаходити потрібне значення сталих для забезпечення заданих параметрів ковзання частинки. Складання диференціальних рівнянь руху ковзання частинки по гвинтовій поверхні здійснювалось в проєкціях на осі нерухомої системи координат. В ролі кривої осьового перерізу поверхні було розглянуто параболу, до рівняння якої входить стала величина. Отримані аналітичні залежності дозволили визначити оптимальні значення сталих у рівнянні кривої осьового перерізу, що забезпечило необхідну швидкість ковзання частинки та відстань від осі гвинтової поверхні. Це відкрило можливості для проєктування гвинтових спусків

з урахуванням специфічних технологічних вимог, зокрема для гравітаційної сепарації або безенергетичного транспортування сипучих матеріалів. Практичне застосування запропонованих розрахунків продемонстровано на прикладі параболічної форми перерізу, що підтверджує ефективність методу для оптимізації кінематичних параметрів руху. У результаті дослідження отримано вирази для проєктування гвинтових гравітаційних спусків та визначено вплив введеної сталої на кінематичні параметри ковзання частинок

Ключові слова: швидкість ковзання; сили ваги; реакції; тертя; гравітаційне транспортування